



Demonstrating Analytical Similarity of Trastuzumab Biosimilar HLX02 to Herceptin[®] with a Panel of Sensitive and Orthogonal Methods Including a Novel FcγRIIIa Affinity Chromatography Technology

Liqi Xie¹ · Erhui Zhang¹ · Yanpeng Xu¹ · Wenyuan Gao¹ · Linlin Wang¹ · Michael Hongwei Xie¹ · Peilan Qin¹ · Lihong Lu¹ · Sipeng Li¹ · Pengcheng Shen¹ · Weidong Jiang¹ · Scott Liu¹

Published online: 18 February 2020
© The Author(s) 2020

Abstract

Background A biosimilar needs to demonstrate its similarity to the originator reference product (RP) in terms of structural and functional properties as well as nonclinical and clinical outcomes.

Objectives The aim was to assess the analytical similarity between the trastuzumab biosimilar HLX02 and Europe-sourced Herceptin[®] (EU-Herceptin[®]) and China-sourced Herceptin[®] (CN-Herceptin[®]) following a quality-by-design (QbD) quality study and tier-based quality attribute evaluation.

Methods A panel of highly sensitive and orthogonal methods, including a novel Fc gamma receptor IIIa (FcγRIIIa) affinity chromatography technique that enables quantitative comparison of glycan effects on effector function, was developed for the assessment. To ensure the full product variability was captured, ten batches of HLX02 were compared with 39 RP batches with expiry dates from August 2017 to March 2021.

Results The extensive three-way similarity assessment demonstrated that HLX02 is highly similar to the RPs. Furthermore, the %afucose, %galactose, and FcγRIIIa affinity of the RPs were observed to first decrease and then return to the original level in relation to their expiry dates, and the RP batches can be subgrouped by their FcγRIIIa affinity chromatograms. HLX02 is demonstrated to be more similar to the RPs of the high FcγRIIIa affinity group.

Conclusion Besides having an overall high analytical similarity to both EU-Herceptin[®] and CN-Herceptin[®], HLX02 is more similar to Herceptin[®] with high FcγRIIIa affinity, a result that demonstrates the power of the novel FcγRIIIa affinity chromatography technology in biosimilarity evaluation.

1 Introduction

Herceptin[®] (trastuzumab) is the first humanized monoclonal antibody (mAb) and the first targeted IgG1 drug approved to treat human epidermal growth factor receptor 2 (HER2)-positive breast cancer by inhibiting ligand-independent

HER2 signaling pathways and inducing antibody-dependent cell-mediated cytotoxicity (ADCC) [1, 2]. Trastuzumab was added into the World Health Organization (WHO) model list of essential medicines in 2015 [3]; however, 60% of patients with HER2-positive breast cancer may not have received this important therapy at some point during their course of treatment [4]. The application of biosimilars would improve affordability and bring increased access to trastuzumab to a broader patient population [5, 6]. By June 2019, the European Medicines Agency (EMA) and the US Food and Drug Administration (FDA), respectively, approved five trastuzumab biosimilars after patent expiration of Herceptin[®] and several new dosage forms. Although no trastuzumab biosimilar has been approved in China yet, the trastuzumab biosimilar HLX02, developed by Shanghai Henlius Biotech, Inc., was granted priority review by the China National Medical Products Administration (NMPA) on July 4, 2019.

Liqi Xie and Erhui Zhang contributed equally.

Electronic supplementary material The online version of this article (<https://doi.org/10.1007/s40259-020-00407-0>) contains supplementary material, which is available to authorized users.

✉ Michael Hongwei Xie
michael_xie@henlius.com; michaelxie68@yahoo.com

¹ Shanghai Engineering Research Center of Anti-tumor Biologic Drugs, Shanghai Henlius Biotech., Inc., Shanghai, China

Key Points

Extensive characterization showed that the %afucose, %galactose, and Fc gamma receptor IIIa (FcγRIIIa) affinity of the trastuzumab reference products decreased and then returned to the original level with respect to their expiry dates from August 2017 to March 2021.

A quality-by-design quality study and tier-based quality attribute assessment demonstrated that HLX02 is highly similar to both China-sourced Herceptin® and EU-sourced Herceptin®, and is more similar to the batches with high FcγRIIIa affinity in particular, in terms of glycan structures and the corresponding biological functions.

Compared to surface plasmon resonance, FcγRIIIa affinity chromatography exhibits higher sensitivity to changes in the FcγRIIIa affinity of trastuzumab, demonstrating the power of this new technology in biosimilarity evaluation.

HLX02 is the first trastuzumab biosimilar accepted for new drug application (NDA) review by the NMPA and the first China-developed antibody and trastuzumab biosimilar accepted for marketing authorization application (MAA) review by the EMA. Herein, an extensive three-way analytical similarity assessment was conducted, following the NMPA [7], EMA [8, 9], US FDA [10, 11], and International Council for Harmonisation of Technical Requirements for Registration of Pharmaceuticals for Human Use (ICH) regulatory guidelines [12] on biosimilarity evaluation. The assessment demonstrated that HLX02 is highly similar to both Europe-sourced Herceptin® (EU-Herceptin®) and China-sourced Herceptin® (CN-Herceptin®). Meanwhile, the characterization results of the reference products (RPs) expiring between August 2017 and March 2021 indicated that the relative abundance of glycoforms (e.g., %afucose and %galactose) and their corresponding Fc gamma receptor (FcγR) binding activities can be subgrouped. Glycoform variations and the resulting lower ADCC have been detected in Herceptin® lots with expiry dates from March 2015 to December 2019 [13, 14]. The Herceptin®-treated patients exposed to those lower-ADCC lots had a significantly lower 3-year event-free survival (EFS) rate (82.5%) than those not exposed (92.5%) [15]. These results highlight the importance of controlling the heterogeneity of glycoforms during biosimilar development of trastuzumab to obtain consistent biological and therapeutic effects. Therefore, further evaluation of the biosimilarity of HLX02 with respect to the RP subgroups is deserved.

ADCC elicited by engagement of immune complexes and FcγRs is one of the major functions of trastuzumab [2]. ADCC is modulated by the structure of Fc glycans [16]. A detailed understanding of the correlation between glycosylation, FcγRIIIa affinity, and ADCC is crucial for managing the effector function of trastuzumab. However, due to the structural heterogeneity of Fc glycans, studies that characterize the overlaying effects of individual glycospecies may lead to contradictory conclusions on whether the glycosylation differences bring about functional changes. Afucosylation is the primary driver of ADCC; dramatically enhanced ADCC activity in IgG has been previously achieved in various studies through the removal of core fucose [17, 18]. Due to the overriding effects of the afucosylated glycoforms, the impact of other sugar residues on ADCC activity is less clear. As a consequence, the presence of glycan types with terminal galactose has been reported to be associated with upregulated, unaffected, or downregulated ADCC activity [16].

Recently, a new technology, FcγRIIIa affinity chromatography [19, 20], was developed to enable quantitative comparison of glycan effects on effector function [21]. By using an FcγRIIIa-immobilized TSKgel FcR-IIIa-NPR column, the novel chromatography is able to separate antibodies according to their affinity to the FcγRIIIa receptor, which conventional surface plasmon resonance (SPR) methods cannot distinguish [22]. The early eluting peaks contain glycoforms with lower FcγRIIIa affinity, while the late eluting peaks contain glycoforms with higher FcγRIIIa affinity, therefore resulting in higher ADCC activity. Further study on the glycoforms of each peak can provide more direct evidence for correlation between glycan structures and FcγRIIIa binding as well as ADCC activity. Therefore, besides a panel of highly sensitive and orthogonal analytical methods applied to assess the analytical similarity between HLX02 and Herceptin®, FcγRIIIa affinity chromatography was used in this study to subgroup Herceptin® batches, defined by their expiry dates, and to compare HLX02 with each subgroup for FcγRIIIa binding. Interestingly, consistent with the glycan distribution differences, the FcγRIIIa binding activity of Herceptin® batches from August 2017 to March 2021 was first down shifted, and then returned to the original level across the monitored RP expiry period. In addition to the overall high similarity of HLX02 to the RPs demonstrated by the extensive three-way similarity assessment following a quality-by-design (QbD) quality study and tier-based quality attribute evaluation, the FcγRIIIa affinity chromatography results further showed that HLX02 is more similar to Herceptin® that has a high FcγRIIIa affinity, with expiry dates before February 2018 or after May 2020, than to the RP with low FcγRIIIa affinity (those lots with expiry dates in between).

2 Materials and Methods

2.1 Materials

Reference product EU-Herceptin[®] (Herceptin[®], 150 mg/vial) and CN-Herceptin[®] (Herceptin[®], 440 mg/vial) were purchased from Roche. HLX02 (150 mg/vial) was manufactured by Shanghai Henlius Biopharmaceuticals, China. Thirteen batches of CN-Herceptin[®], 26 batches of EU-Herceptin[®], and ten batches of HLX02 were chosen to cover a range of shelf lives. Their corresponding lot numbers and expiry dates are listed in Supplemental Table 1 [see the electronic supplementary material (ESM)]. Each sample was reconstituted following the manufacturer's instructions, and stored in multiple aliquots at -80°C before expiration to avoid repeating freeze/thaw cycles. Chemicals were all purchased from Sigma Chemical Co. without special mention.

2.2 Primary Structure Analysis

Following a previous study [23], the molecular weights of intact, reduced, and papain-cleaved mAb as well as reduced/non-reduced peptide mapping were analyzed using a Waters ACQUITY ultra performance liquid chromatography (UPLC) system coupled online to a Waters Xevo G2-XS Q-TOF mass spectrometer. The free thiol groups in the samples were determined by a Measure-iT thiol assay kit (Thermo Fisher).

The amino acid composition of HLX02 and the RPs was determined using an acid hydrolysis method. Briefly, protein samples were desalted, mixed with 2-aminobutyric acid (AABA) and hydrolyzed with 7 M of HCl and 1% phenol to get free amino acids. The amino acids were dried and labeled with an AccQ Fluor kit (Waters), and separated by reversed-phase high-performance liquid chromatography (RP-HPLC) (AccQ Tag Ultra C18 column, 1.7 μm , 2.1 \times 100 mm, Waters). The molar concentration of each amino acid was determined by an internal standard method.

2.3 Oligosaccharide Analysis

As previously described [23], the N-linked oligosaccharides were enzymatically released, labeled by RapiFluor-MS N-Glycan kit (Waters), and analyzed by hydrophilic interaction UPLC with fluorescence detection (HILIC UPLC-FLD). The content of sialic acid in the mAb samples was analyzed by RP-HPLC after labeling with 1,2-diamino-4, 5-methyleoxybenzene (DMB) (Takara).

Monosaccharides were hydrolyzed with 15.4% trifluoroacetic acid (TFA) from desalted protein samples, and analyzed by ion chromatography (ICS 5000+, Thermo Scientific) using an anion exchange column (Dionex Carbo Pac[™] PA 10, 10.0 μm , 4.0 \times 250 mm, Thermo Scientific) coupled with an AminoTrap column (Dionex[™], 10.0 μm , 4.0 \times 50 mm, Thermo

Scientific). The concentration for each monosaccharide was determined by corresponding monosaccharide standards.

2.4 Higher Order Structure Analysis

Thermal stability profiles were determined using differential scanning calorimetry (DSC). Secondary and tertiary structures were measured by multiple advanced spectroscopy methods such as circular dichroism (CD) absorption spectra, and Fourier transform infrared spectroscopy (FTIR) spectra, acquired as previously described [23]. In fluorescence spectrum (FLR) measurements, samples were diluted to 1 mg/mL and then analyzed by a Molecular Devices SpectraMax i3X equipped with a fluorescence detector (excitation/emission light: 275 nm/300–500 nm). After being supplemented with 10% D₂O, the protein nuclear magnetic resonance (¹H NMR) spectra of mAb samples were recorded at 303 K on a Bruker 800-MHz spectrometer equipped with a triple-resonance cryoprobe.

2.5 Assays for Heterogeneities due to Charge and Size Variants and for Bioprocess Residual Impurities

Charge variants, size variants, and process-related impurities, including residual host cell proteins (HCPs), protein A and host cell DNA, were evaluated using the same methods as described in the previous study [23]. The content of corresponding variants was evaluated by determining the peak area of each species as a percentage of the total peak area.

Sedimentation velocity analytical ultracentrifugation (SV-AUC) experiments were carried out on a Beckman Coulter Optima XL-I Analytical Ultracentrifuge using both interference and absorbance detection. Samples were filled in titanium cuvettes with an optical path length of 12 mm. The experiments were performed at 20 $^{\circ}\text{C}$. An angular velocity of 40 krpm was applied.

2.6 Particle Analyses

The size distribution profile of submicron particles was performed using dynamic light scattering (DLS). The hydrodynamic diameter of samples was determined using a Zetasizer Nano ZS instrument (Malvern Panalytical). The scattered light was monitored at 173 $^{\circ}$ to the incident beam; 100 μL of sample was loaded to the well and run in triplicates. The hydrodynamic diameter data were collected upon adequate equilibration at 25 $^{\circ}\text{C}$. Finally, the mean size of particles (Z-Ave) was determined by the photon auto-correlation function.

Sub-visible particles were measured using an MFI-5200 Flow Microscope Series (Protein Simple). Images of individual particles were captured and analyzed by the system software (MVSS software) to extract each particle and to

compile a database containing particle counts and sizes. The sub-visible particle amount in the equivalent circular diameter (ECD) over 10 and 25 μm was reported.

2.7 C1q and Fc Receptor Binding Assays

Following the previous study [23], the binding activity with respect to human C1q was determined by enzyme-linked immunosorbent assay (ELISA), and the affinity of mAb samples for human Fc γ and neonatal Fc receptor (FcRn) receptors was analyzed by SPR with a Biacore T200 instrument (GE Healthcare).

In Fc γ RIIIa affinity chromatography analysis, 50 mM citric acid at pH 6.5 was used as mobile phase A, and 50 mM citric acid at pH 4.0 as mobile phase B. The samples were diluted to 1.0 mg/mL with mobile phase A, and analyzed by a linear gradient of buffer B (0–100%) at a flow rate of 1.0 mL/min for 35 min applied to the Fc γ RIIIa affinity column (4.6 mm I.D. \times 75 mm, TOSOH), equipped on an Agilent 1260 HPLC system.

2.8 Fc-Effector Function Bioassays

Biological activities were measured in cell lines by evaluating the cytotoxicity in the presence of HLX02, EU-Herceptin[®], or CN-Herceptin[®]. ADCC was evaluated by colorimetric luciferase release assay. NFAT-CD16a Jurkat cells, which constitutively express CD16a and nuclear factor of activated T cells (NFAT) luciferase, were used as effector cells. The HER2-overexpressing cell line BT-474 was used for the target cells. In the ADCC assay, BT-474 cells (1.0×10^4) and NFAT-CD16a Jurkat cells (1.0×10^5) were seeded in a 96-well plate and incubated with fourfold serial dilution of mAbs at a concentration from 7500 to ~ 0.03 ng/mL. After incubation at 37 °C, 5% CO₂ for 6 h, cell cytotoxicity was measured by quantification of released luciferase-detecting luminescence with Bio-Glo[™] Luciferase Assay Reagent (Promega), following the manufacturer's instructions, and reported as ADCC activity.

To assess complement-dependent cytotoxicity (CDC) activity, BT-474 cells were incubated with twofold serially diluted mAbs (2 $\mu\text{g}/\text{mL}$ –31 ng/mL) in the presence of normal human serum as a complement source. After incubation for 0.5 h at 37 °C in 5% CO₂, CDC activity was monitored by determining cell viability, reading the absorbance at 450 nm (OD450) with CCK8 reagent (Dojindo). The anti-proliferation assay was performed in BT-474 cells using different concentrations of mAbs (15 $\mu\text{g}/\text{mL}$ –29.297 ng/mL) for incubation at 37 °C in 5% CO₂ for 72 h. The apoptosis bioassay measured the trastuzumab-induced externalization of phosphatidylserine in BT-474 cells. Briefly, BT-474 cells were treated with twofold serially diluted mAbs at a

concentration from 7500 to 0 ng/mL at 37 °C in 5% CO₂ for 72 h. Apoptosis efficiency was analyzed by apoptosis kit (Promega) according to the manufacturer's instructions. Relative potency was determined using a parallel logistic assay by comparing the half maximal effective concentration (EC50) of the reference sample to the test sample.

2.9 HER2 Binding Assay

The binding affinity of HLX02, EU-Herceptin[®], and CN-Herceptin[®] with respect to HER2 was measured using both SPR and ELISA. For ELISA, recombinant human HER2 protein was coated onto the wells of microtiter plate and incubated with a dose titration of mAbs (from 1.016 ng/mL to 20,000 ng/mL). For SPR, HER2 protein was immobilized on the surface of a CM5 chip flow cell followed by injection of serial diluted mAbs over flow cells. The HER2 binding activity of mAbs was determined by the dissociation constant (K_D) or EC50 of the reference sample compared to the test sample.

2.10 Forced Degradation Studies

The forced degradation behaviors and trends were investigated under the following stress conditions: higher temperature (50 °C), light exposure (4500 \pm 500 lux), strong acid (pH 4), strong alkali (pH 10), strong oxidizer (1.0% tert-butyl hydroperoxide (tBHP)) or shaking at a speed of 1000 rpm at 25 °C. The pulling time schedule and subsequent characterization of the degradation samples using a panel of stability indicative assays are listed in Supplemental Table 2 (see the ESM).

2.11 Statistical Analysis

The quality attributes of trastuzumab were ranked according to the potential impact on clinical efficacy and safety following the QbD quality study and extensive characterization of the RPs. The standard deviation (SD) of the RPs is used to determine similarity acceptance criteria. Equivalence testing was applied for attributes ranked as tier 1, those with the highest potential clinical impact. An interval (-1.5 SD, $+1.5$ SD) that can support a 90% confidence interval was applied in two one-sided tests to determine the similarity of HLX02 and the RPs. A quality range approach was employed for attributes categorized as tier 2, those with a moderate risk ranking. Similarity to the RP can be determined when 90% of HLX02 data falls into the quality range (mean -3 SD, mean $+3$ SD). Tier 3 attributes, those with the lowest risk ranking, were evaluated by visual comparison. The qualitative result of any test was evaluated by visual comparison also, regardless of its risk ranking.

3 Results

To compare the structural and functional properties of HLX02 with CN-Herceptin[®] and EU-Herceptin[®], a set of highly sensitive, orthogonal, and state-of-the-art analytical techniques (Table 1) for characterization of the primary structure, higher order structure, heterogeneities due to glycosylation, molecular size and charge variants, immunological and biological activities, bioprocess residuals, and forced degradation behaviors were employed in the study of the quality attributes that could impact the purity, potency, safety, and efficacy of trastuzumab. After extensive characterization of the RPs and evaluation of critical quality attributes following a QbD strategy [24, 25], each quality attribute was assigned to one of the three tiers, in line with regulatory suggestions [10, 24, 26]. The similarity range for each quality attribute analyzed by specific methods was set following the tier-based approach.

In addition, based on the comprehensive characterization of Herceptin[®] expiring between August 2017 and March 2021, each quality attribute of the RPs was examined to see if it changed along with the expiration date. The similarity assessment of HLX02 with respect to the RPs was also evaluated across the monitored expiration dates of the RPs.

3.1 HLX02 has the Same Amino Acid Sequence as the RPs and Exhibits Highly Similar Primary and Higher Order Structures to the RPs, Especially Those with a Higher Level of Galactosylation

The primary structure of HLX02, CN-Herceptin[®], and EU-Herceptin[®] was characterized and compared by a series of advanced mass spectrometry (MS)-based analyses and a free thiol fluorescent detection kit (Table 1). First of all, HLX02 has the same amino acid sequence as the RPs and consistent 100% coverage of the theoretical protein sequences of trastuzumab, demonstrated by liquid chromatography–tandem mass spectrometry (LC–MS/MS) peptide mapping of alternative trypsin and chymotrypsin digests and backed by amino acid analysis. The same post-translational modification (PTM) types/sites and highly similar site occupancies were determined among all the products (Fig. 1a, Supplemental Table 3 in the ESM). Secondly, LC–MS/MS analysis of trypsin-digested non-reduced samples showed the same disulfide linkages of the IgG1 subtype in HLX02 and the RPs without a mismatched disulfide bond (Supplemental Table 4). The result was supported by the finding that the number of free thiol groups on HLX02 and the RPs was below the limit of quantification (0.688 $\mu\text{mol/mL}$). Finally, the molecular weight analyses demonstrated the same mass species and highly similar primary structures between

HLX02 and the RPs, and indicated some intensity variations of glycan moieties among the RP batches (Fig. 1b, c; Supplemental Figure 1). In accordance with previous findings [13], the content of galactosylated glycoforms in some batches of the RP was quite different from the others and relatively lower. Although same mass species were identified from all the examined samples, the intact MS profiles of HLX02 were more similar to those RPs with higher levels of galactosylated glycans (i.e., G1F and G2F, as shown in Fig. 1b). The MS spectra of reduced heavy chains (HCs) further confirmed the observation (Fig. 1c). This was further investigated later in this study.

The higher order structures that are vital for the biological activity, safety, and stability of therapeutic proteins are highly similar between HLX02 and the RPs. The DSC, CD, FLR, FTIR, and 1D ¹H NMR spectra of all examined samples are visually similar, as shown in Fig. 1d–f and Supplemental Figures 2 and 3.

3.2 HLX02 has Highly Similar Purity and Impurities to the RPs, Except for Slightly Lower Levels of HC D102-Isomerization Variant, Aggregates, and Non-glycosylated HCs

Charge variants of HLX02 and the RPs were detected by imaged capillary isoelectric focusing (icIEF) and cation exchange chromatography (CEX). Similar icIEF profiles and the same isoelectric point (pI) of 9.0 in all products were observed (Supplemental Figure 4 in the ESM). The CEX profiles of HLX02, EU-Herceptin[®], and CN-Herceptin[®] were also highly similar, and no unique CEX peaks were detected in any of the products (Fig. 2a). Meanwhile, a slightly smaller amount of the Asp isomerization variant of HC D102 (peak 4) was observed in HLX02 (mean 5.4% vs. 6.5%) (Supplemental Table 5). Consistent with previous research [27], peak 4 has lower biological activity, while the other acidic and basic peaks have no significant change in bioactivity compared with the main peak (data not shown). Therefore, the lower level of D102 isomerization in HLX02 is beneficial to the efficacy and safety of trastuzumab.

HLX02 and Herceptin[®] showed similar high levels of purity; HLX02 has a slightly lower level of aggregates and non-glycosylated HC (NGHC) compared with the RPs. The size-exclusion chromatography (SEC) chromatograms and capillary electrophoresis–sodium dodecyl sulfate (CE-SDS) profiles were highly similar among HLX02, EU-Herceptin[®], and CN-Herceptin[®], and no unique species were detected in any of the products (Fig. 2b, c). Monomer was the dominant component in all the chromatograms, indicating low levels of impurities in all the products. Compared with the RPs, a slightly lower level of aggregates was observed for HLX02 (mean 0.3% vs. 0.5%), demonstrating the success of

Table 1 Analytical methods used for evaluating similarity of HLX02 biosimilar to its innovator Herceptin®

Test classification	Quality attributes	Tier	Methods	Demonstrated similarity	
Physicochemical properties and purity					
Primary structure	Amino acid sequence	I	Reduced peptide mapping by LC-MS/MS	Identical to the RP	
		III	Amino acid analysis by RP-UPLC	Similar to the RP	
	Molecular weight of intact, reduced antibody and subunits	II	Intact protein mass analysis by LC-MS	Same mass species	
		II	Reduced protein mass analysis by LC-MS		
		II	Reduced and deglycosylated mass analysis by LC-MS		
		II	Papain digested protein subunit mass analysis by LC-MS		
	Disulfide linkage	II	Non-reduced peptide mapping by LC-MS/MS	Identical to the RP	
	Free thiols	II	Free thiol fluorescent detection kit	Similar to the RP	
	PTMs	II	Reduced peptide mapping by LC-MS/MS	Similar to the RP	
	Glycosylation site	II	Deglycosylated and reduced peptide mapping	Identical to the RP	
Higher order structure	Secondary and tertiary structure	III	DSC	Similar to the RP	
			CD		
			FLR		
			FTIR		
			NMR		
Charge variants	Charge variants	II	CEX	Similar to the RP; slightly less peak 4	
	Isoelectric point	II	icIEF	Identical to the RP	
Size variants	Aggregates, monomers, LMWs and NGHC	II/III	SEC-HPLC	Similar to the RP; slightly less aggregates and NGHC	
			Reduced and non-reduced CE-SDS		
			SEC-MALS		
			SV-AUC		
Glycosylation	Glycan distribution	II	HILIC UPLC-FLD	Similar to the RP; slightly higher sialylation, not clinically meaningful	
	Sialic acid	II	RP HPLC-FLD		
	Monosaccharide analysis	III	Ion chromatography		
Functional assays					
Immunochemical properties	FcRn, FcγR (FcγRIa, FcγRIIa, FcγRIIb/c, FcγRIIIa (V), FcγRIIIa (F), FcγRIIIb)	II	SPR	Similar to the RP	
		II	FcγRIIIa affinity chromatography	Similar to the RP	
		III	ELISA	Similar to the RP	
Bioactivity	HER2 binding	I	ELISA	Similar to the RP	
			SPR	Similar to the RP	
	Anti-proliferation	I	Cell-based assay	Similar to the RP	
	Apoptosis	II	Cell-based assay	Similar to the RP	
	ADCC	I	Cell-based assay	Similar to the RP	
	CDC	III	Cell-based assay	Similar to the RP, both negative	
	Process-related impurities	DNA	I	qPCR	Similar to the RP
		HCP	I	ELISA	Similar to the RP
Protein A		I	ELISA	Similar to the RP	

Table 1 (continued)

Test classification	Quality attributes	Tier	Methods	Demonstrated similarity
Particles	Sub-micro particles	III	DLS	Similar to the RP
	Sub-visible particles	III	MFI	Similar to the RP

ADCC antibody-dependent cell-mediated cytotoxicity, *CD* circular dichroism, *CDC* complement-dependent cytotoxicity, *CE-SDS* capillary electrophoresis–sodium dodecyl sulfate, *CEX* cation exchange chromatography, *DLS* dynamic light scattering, *DSC* differential scanning calorimetry, *ELISA* enzyme-linked immunosorbent assay, *FcγR* Fc gamma receptor, *FcRn* neonatal Fc receptor, *FLR* fluorescence spectrum, *FTIR* Fourier transform infrared spectroscopy, *HCP* host cell protein, *HER2* human epidermal growth factor receptor 2, *HILIC UPLC-FLD* hydrophilic interaction–ultra performance liquid chromatography–fluorescence detection, *icIEF* imaged capillary isoelectric focusing, *LC-MS/MS* liquid chromatography tandem mass spectrometry, *LMWs* low molecular weight variants, *MFI* micro-flow imaging, *NGHC* non-glycosylated heavy chain, *NMR* nuclear magnetic resonance, *PTMs* post-translational modifications, *qPCR* quantitative real-time polymerase chain reaction, *RP* reference product, *RP HPLC-FLD* reversed-phase high-performance liquid chromatography–fluorescence detection, *RP-UPLC* reversed-phase ultra performance liquid chromatography, *SEC-HPLC* size-exclusion chromatography–high-performance liquid chromatography, *SEC-MALS* size-exclusion chromatography with multi-angle light scattering, *SPR* surface plasmon resonance, *SV-AUC* sedimentation velocity analytical ultracentrifugation

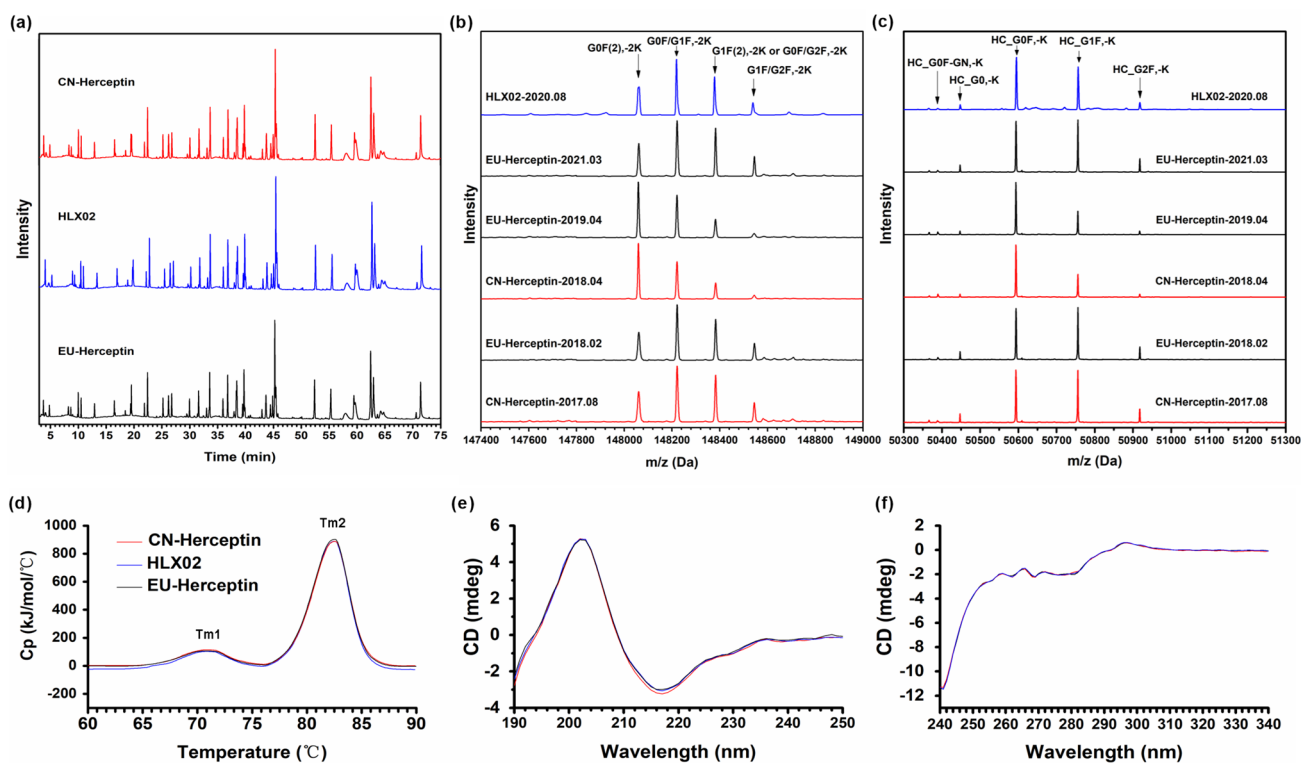


Fig. 1 Primary and higher order structure of representative HLX02, CN-Herceptin®, and EU-Herceptin®. **a** Peptide maps of tryptic digests; mass spectra of **b** intact mAb and **c** reduced HC; **d** DSC thermograms; **e** far-UV CD spectra and **f** near-UV CD spectra. The

mass spectra of the RPs in diagrams **b** and **c** are plotted in the order of expiry date. *CD* circular dichroism, *CN* China-sourced, *DSC* differential scanning calorimetry, *EU* Europe-sourced, *HC* heavy chain, *mAb* monoclonal antibody, *RP* reference product

the HLX02 process (Supplemental Table 6; see the ESM). SV-AUC results further confirmed the observation (Supplemental Table 7). CE-SDS was used as an orthogonally complementary approach to accurately analyze fragments and NGHCs of the mAbs (Supplemental Table 8). Besides demonstrating highly similar profiles with respect to size variants, reduced CE-SDS indicated relatively lower levels of NGHCs for HLX02 compared to the RPs.

HLX02 has similarly low levels of sub-visible particles compared with the RPs, as assessed by micro-flow imaging (MFI). The particle sizes of major submicron particles in HLX02, CN-Herceptin®, and EU-Herceptin® are similar, as assessed by DLS (see Supplemental Table 9 in the ESM).

The process-related impurities are at similarly low levels in all the product lots (Supplemental Table 10). Residual

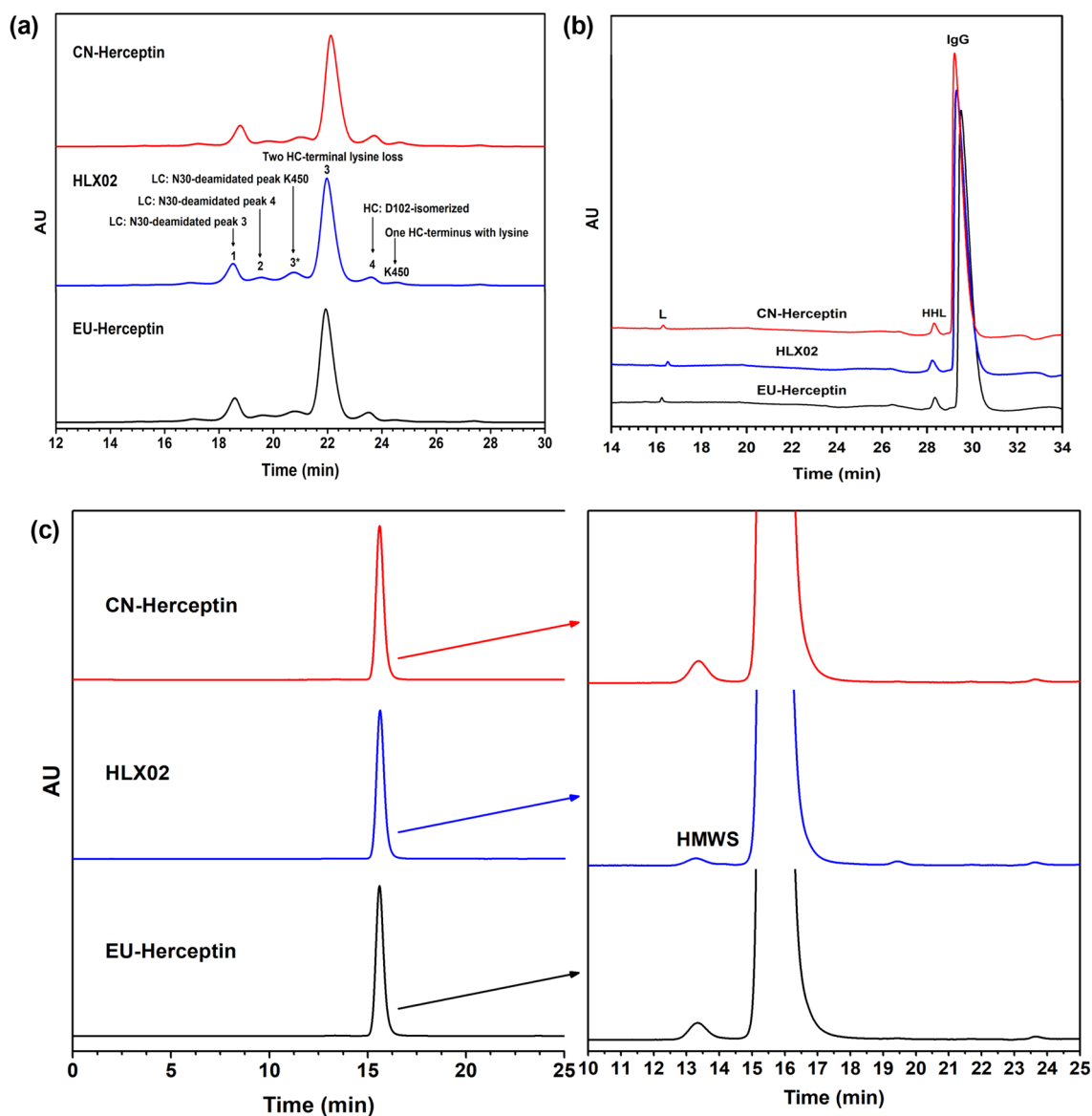


Fig. 2 Size and charge variants of HLX02, CN-Herceptin[®], and EU-Herceptin[®] assessed by **a** CEX-HPLC, **b** non-reduced CE-SDS, and **c** SEC-HPLC. *CE-SDS* capillary electrophoresis–sodium dodecyl sulfate, *CEX* cation exchange chromatography, *CN* China-sourced, *EU*

Europe-sourced, *HPLC* high-performance liquid chromatography, *SEC-HPLC* size-exclusion chromatography–high-performance liquid chromatography

HCP, protein A, and host cell DNA were all less than 2 ng/mg, 1 ng/mg, and 0.05 pg/mg, respectively.

In summary, HLX02 and the RPs have similarly high purity and similar levels of charge variants, size variants, particles, and low bioprocess residuals. Furthermore, the lower percentages of aggregates and NGHC in HLX02 indicated the high product quality and the success of its manufacturing process.

3.3 HLX02 and the RPs Showed Good Stability and Consistent Degradation Behaviors

Product degradation trends can be determined by forced degradation studies, providing supplemental evidence for similarity assessment, and such studies can detect the potential slight differences between HLX02 and the RPs that cannot be detected in normal structural characterization. Forced

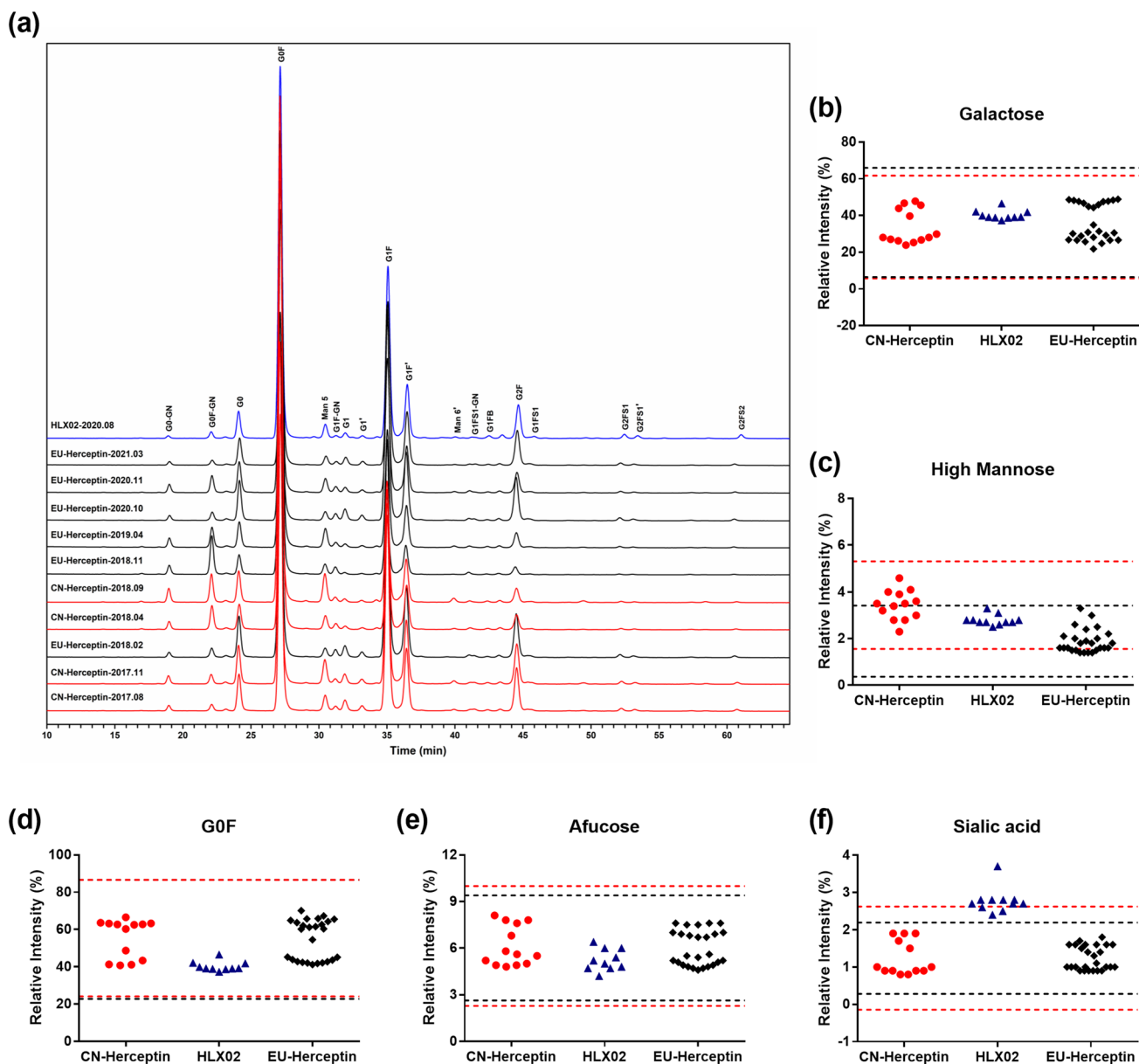


Fig. 3 Comparison of glycan structures released from HLX02, CN-Herceptin[®], and EU-Herceptin[®] by PNGase F. **a** N-glycan profiles by HILIC UPLC-FLD; the major types of glycans are labelled beside the corresponding peaks in the *top panel* (HLX02). **b–f** Quantitative

results of each glycoform subtype analyzed using tier 2 attribute criteria (mean \pm 3 SD). *CN* China-sourced, *EU* Europe-sourced, *HILIC UPLC-FLD* hydrophilic interaction–ultra performance liquid chromatography–fluorescence detection, *SD* standard deviation

degradation studies under higher temperature, illumination, acidity, alkalinity, oxidation, and shaking were conducted. Highly similar degradation behaviors and degradation trends were observed for HLX02, EU-Herceptin[®], and CN-Herceptin[®]. As an example, the changing trends of CEX components (acidic, main, peak 4, and basic peaks) are illustrated in Supplemental Figure 5 (see the ESM).

3.4 The Relative Abundance Difference of Glycoforms Between HLX02 and the RPs is Smaller than the Variability Among Different Batches of the RPs

The glycoform profiles of HLX02 and the RPs detected by HILIC UPLC-FLD showed identical glycoform species among all the products (Fig. 3) and comparable profiles. High similarity was observed in glycan groups (see Supplemental Table 11 in the ESM) for the relative abundance

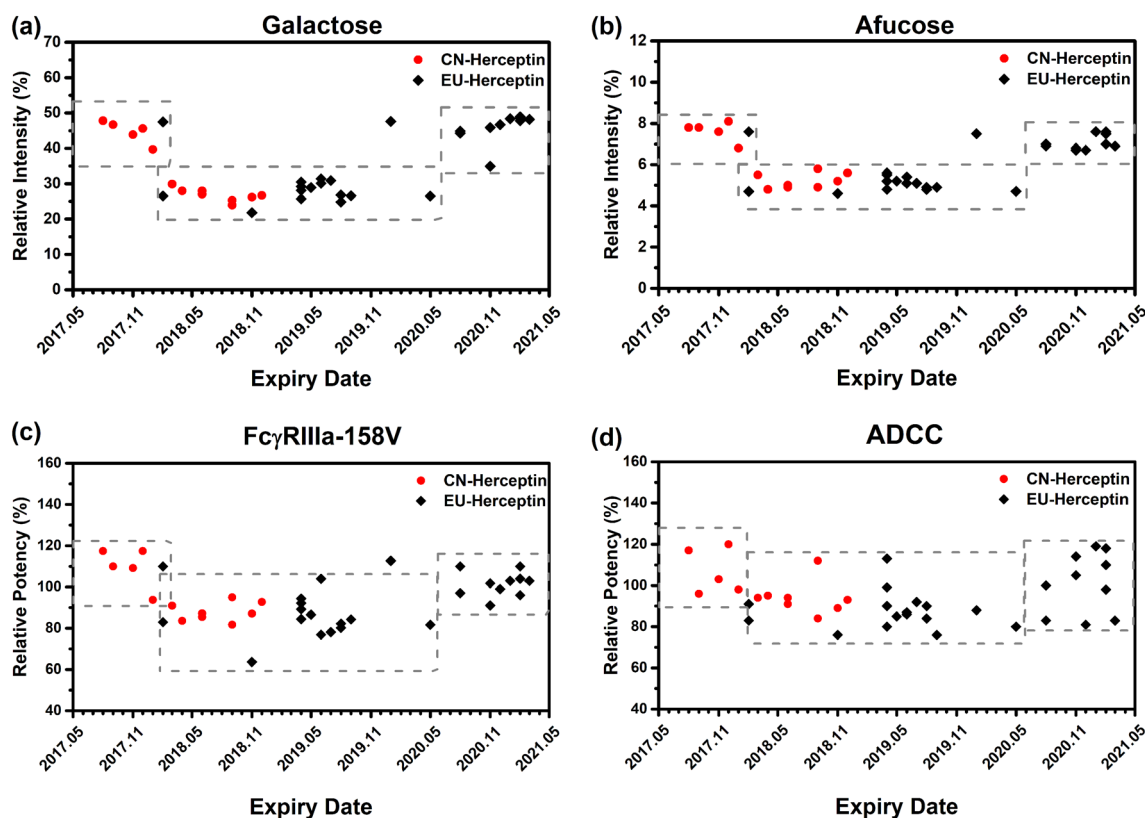


Fig. 4 Percentages of N-glycans and the corresponding bio-functions related to expiry date of the examined RPs. **a** %Galactose and **b** %afucose, **c** Fc γ RIIIa-158V binding activity by SPR, and **d** ADCC

activity. ADCC antibody-dependent cell-mediated cytotoxicity, Fc γ R Fc gamma receptor, RP reference product, SPR surface plasmon resonance

of GOF and high mannosylation, galactosylation, and afucosylation of HLX02 compared to the RPs, except for a slightly higher sialylation content for HLX02 (mean 2.8% vs. 1.2%) (Fig. 3; Supplemental Table 11). The observation was orthogonally confirmed by monosaccharide analysis by ion chromatography. Despite the low amounts expected to be present, absolute quantification of sialic acid was performed to further characterize the glycan structures. The content of *N*-acetylneuraminic acid (NANA) in HLX02 and the RPs was 0.087–0.137 mol/mol and 0.028–0.061 mol/mol, respectively. *N*-glycolylneuraminic acid (NGNA), which may cause potential immunogenicity, was not detected in HLX02, while trace amounts of NGNA (0.002–0.005 mol/mol) were detected in the RPs (Supplemental Table 11). The marginally higher NANA content in the HLX02 lots is not expected to lead to safety issues or to induce a clinical meaningful difference, as demonstrated by a series of key functional assays shown below.

Relatively large variations in glycan distribution among different RP batches were observed, broader than those of HLX02 and between HLX02 and the RPs. This is consistent with the observation of intact and reduced LC–MS analyses described above for the relative MS intensity

difference of glycoforms. The relative content of afucosylated, galactosylated, high mannose, and sialylated glycan types in the RP batches was 4.6–7.6%, 21.8–48.9%, 1.4–3.6% and 0.8–1.9%, respectively. Glycan distribution among the RP batches was observed to shift along with the expiry dates from March 2017 to March 2021 (Fig. 4a, b). Although the relative content of the high mannose type of glycans (%HM) was relatively steady in EU-Herceptin[®], there was a marked downward drift of %afucose and %galactose starting at lots with expiry dates from February 2018, and a subsequent return to the original levels for the batches expiring after May 2020. %Glycan of the RPs can be subdivided into three groups from the expiry time dimension, and into two groups at relative content level, according to %afucose or %galactose. The effect of the above %glycan drifts was further investigated by functional studies (Fig. 4c, d).

3.5 Biological and Immunological Activities are Similar Between HLX02 and the RPs

The biological and immunological similarity of HLX02 compared with EU-Herceptin[®] and CN-Herceptin[®] was

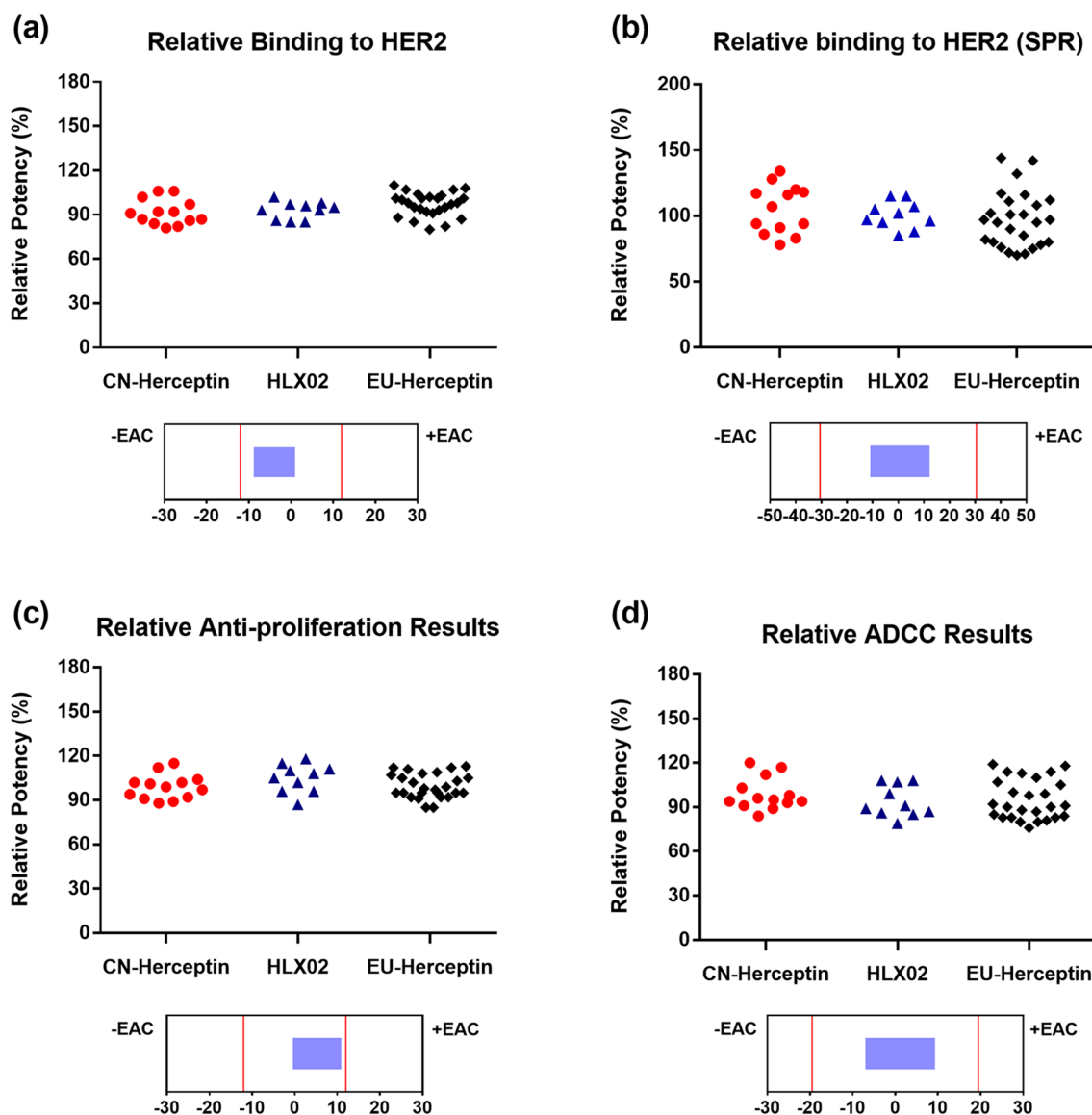


Fig. 5 Scatter plots and equivalence test results for tier 1 bio-functional quality attributes. The dot plots of **a** HER2 binding affinity by ELISA, **b** HER2 binding affinity by SPR, **c** anti-proliferation activity, and **d** ADCC activity were plotted above corresponding equivalence

test results showing 90% CI. ADCC antibody-dependent cell-mediated cytotoxicity, CI confidence interval, ELISA enzyme-linked immunosorbent assay, HER2 human epidermal growth factor receptor 2, SPR surface plasmon resonance

assessed using multiple assays to measure both the target binding (Fab-mediated) and effector (Fc-mediated) functionality of the antibody. HER2 binding (measured by both ELISA and SPR), anti-proliferation, and ADCC might have direct impacts on the primary mechanism of action and were assessed as tier 1 attributes using a statistical equivalence test (Fig. 5). HLX02 met the statistical equivalence criteria and thus showed high similarity to the RPs in all the tier 1 activities. FcγR bindings and the FcRn binding

of HLX02 and the RPs, measured using SPR-based assays, were assessed as tier 2 attributes, using quality ranges ($\text{mean} \pm 3 \text{ SD}$). Similar binding affinities to FcRn, FcγRIa, FcγRIIa, FcγRIIb/c, FcγRIIIa-158F, FcγRIIIa-158V, and FcγRIIIb receptors were observed among all the products (Fig. 6). The apoptosis assay, a secondary mechanism of action assessed as a tier 2 attribute, was also evaluated to be highly similar between HLX02 and the RPs (Fig. 6h). Overexpression of membrane-bound complement regulatory

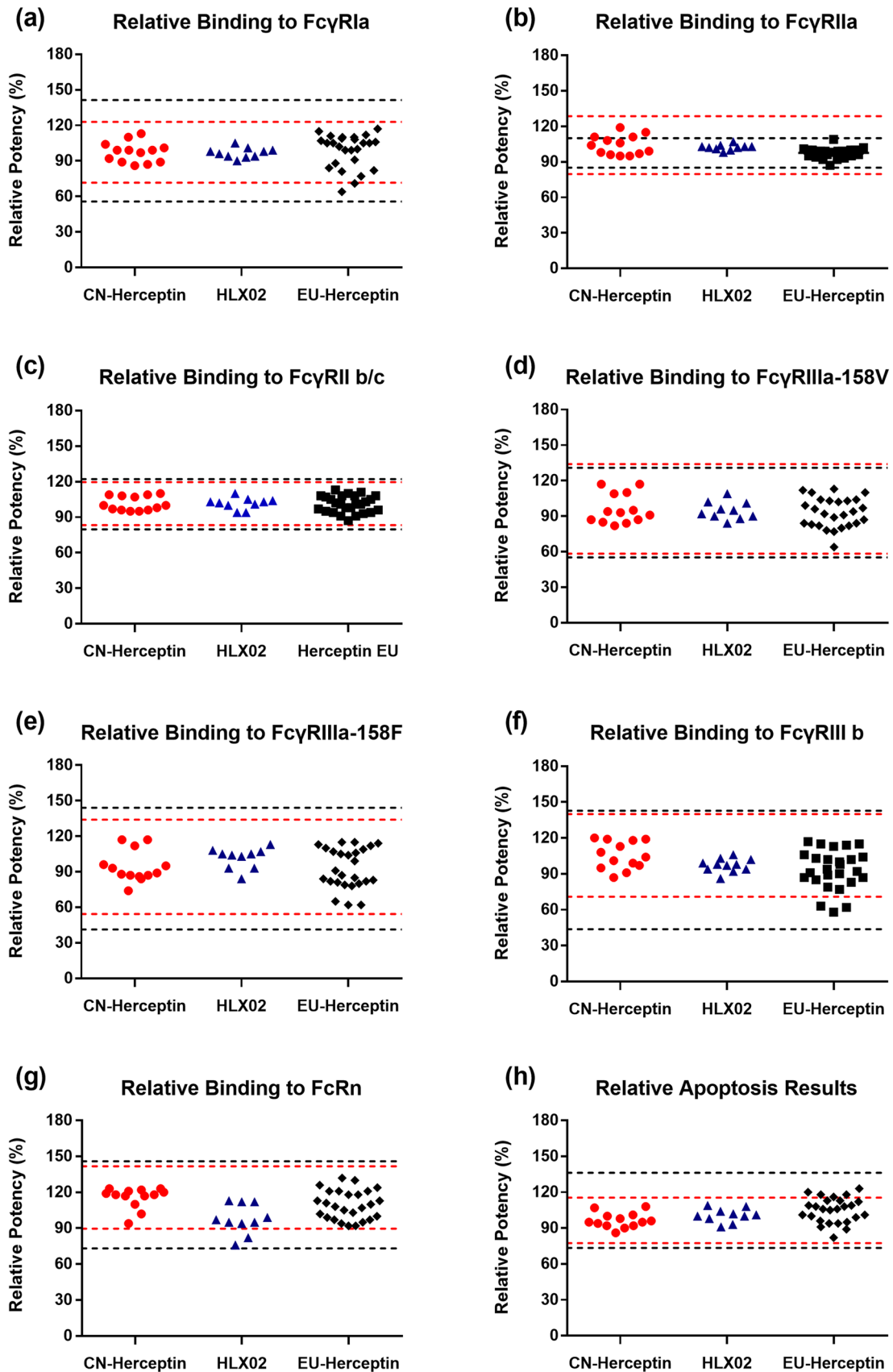


Fig. 6 Comparison of tier 2 bio-functional quality attributes for HLX02, CN-Herceptin[®], and EU-Herceptin[®]. Dot plots of **a** FcγRIa binding affinity, **b** FcγRIIa binding affinity, **c** FcγRIIb/c binding affinity, **d** FcγRIIIa-158V binding affinity, **e** FcγRIIIa-158F binding affinity, **f** FcγRIIIb binding affinity, **g** FcRn binding affinity, and **h** apoptosis. Red and black dash lines represent quality ranges of CN-Herceptin[®] and EU-Herceptin[®], respectively. *CN* China-sourced, *EU* Europe-sourced, *FcγR* Fc gamma receptor, *FcRn* neonatal Fc receptor

protein in HER2-overexpressing breast cancer cells inhibited trastuzumab-induced CDC [28]. Accordingly, binding to the complement cascade component protein, C1q, and CDC were assessed as tier 3 attributes. HLX02-induced CDC was not observed, the same negative result as seen for the RPs. Visually similar C1q binding between HLX02 and the RPs can be easily seen in Supplemental Figure 6 (see the ESM).

In addition to the overall functional comparison, to assess whether %glycan variations as described above had an effect on biologic properties, the functional activity data of each RP batch was examined along with its expiration date. In general, there was little difference in activity among batches, as the activities of most of the RP batches fell within the 80–120% potency range of the reference standard. Most biological activities, including anti-proliferative potency, HER2 binding, and apoptosis, did not show evident changing trends along with the expiry date. But variations in the N-glycan distribution affected affinity with respect to FcγR binding. Similar to the %afucose and %galactose drifts, FcγRIIIa-V158 binding activity was down shifted in the RP batches expiring between February 2018 and May 2020, and return to the original level in the RP batches expiring after May 2020 (Fig. 4c). Being associated with Fc effector binding to FcγR, the ADCC activity of the RP batches with down shifted FcγRIIIa binding activity was slightly lower than that of the RP batches with high FcγRIIIa binding activity (Fig. 4d), despite no statistical change trends being observed throughout the entire range of expiry dates monitored.

3.6 FcγRIIIa Affinity of the RPs can be Subgrouped Along with Expiry Date, and HLX02 is More Similar to the RPs with High FcγRIIIa Affinity

An FcγRIIIa immobilized chromatography column was used to clarify the relationship between binding affinity and glycoforms. The FcγRIIIa affinity chromatography separated trastuzumab into three major peaks (peak 1–3), reflecting an increasing affinity with respect to FcγRIIIa (Fig. 7a). According to the N-glycan profiling of the three peaks, the increase of %afucose and %galactose of trastuzumab enhanced its affinity for FcγRIIIa (Fig. 7b). %Galactose exhibited the strongest correlation with FcγRIIIa affinity (correlation coefficient 0.99). %HM and %sialylation showed no significant correlation with FcγRIIIa affinity activity in this study. The relative peak area of every investigated

sample was plotted against its expiry date, as shown in Fig. 7c. Peak 1, representing low FcγRIIIa affinity species, was up shifted in the RP batches with expiry dates between February 2018 and May 2020, while peak 2 and peak 3, containing the high FcγRIIIa affinity species, were down shifted in the abovementioned RP batches. In addition, the trends of peak 2 and peak 3 perfectly reproduced the trends of %afucose and %galactose changes. These results provided further evidence that the galactosylated and afucosylated glycans could enhance FcγRIIIa binding affinity. In addition, as indicated in Fig. 7c, HLX02 is more similar to the RP batches with higher peak 2 and peak 3.

Based on FcγRIIIa affinity chromatograms, the RPs can be divided into two groups showing high or low FcγRIIIa binding affinity by clustering analysis (Fig. 8a). The trastuzumab batches within the high-affinity group have higher later-elution peaks, corresponding to an increasing affinity with respect to FcγRIIIa, and therefore having greater ADCC activity. Consistent with the FcγRIIIa chromatography results, SPR analysis of the RPs in the low-affinity group exhibited lower FcγRIIIa V/F binding activity than those in the high-affinity group. Similarly, a slight decrease in average ADCC activity (statistically insignificant) was observed in the RPs of the low-affinity group. However, the affinity discrepancies between the RP samples of the two groups could only be discriminated by FcγRIIIa chromatography in the quality range assessment (Fig. 8b), not by SPR. This indicated that FcγRIIIa chromatography is more sensitive to changes in the functional activities of trastuzumab, compared with the traditional SPR-based binding method. According to the similarity assessment results shown in Fig. 8b, it can be inferred that HLX02 is more similar to the RPs with high FcγRIIIa affinity, those having expiry dates before February 2018 or after May 2020.

4 Discussion

The comprehensive three-way analytical similarity assessment demonstrated that HLX02 is highly similar to both CN-Herceptin[®] and EU-Herceptin[®]. The amino acid sequence is identical, and the higher order structures (including secondary and tertiary structures), purity, and product variants are highly similar between HLX02 and Herceptin[®], except for minor differences in the relative abundance of the charge variants and glycan moieties. The slightly lower levels of the HC D102-isomerization variant, aggregates, and NGHC in HLX02 might be beneficial to the product's effectiveness and safety. The difference in glycoform relative abundance observed in HILIC UPLC-FLD glycan profiles between the RP and HLX02 is smaller than the variability among the different RP batches (as defined by their different expiry dates). The slightly higher NANA level observed

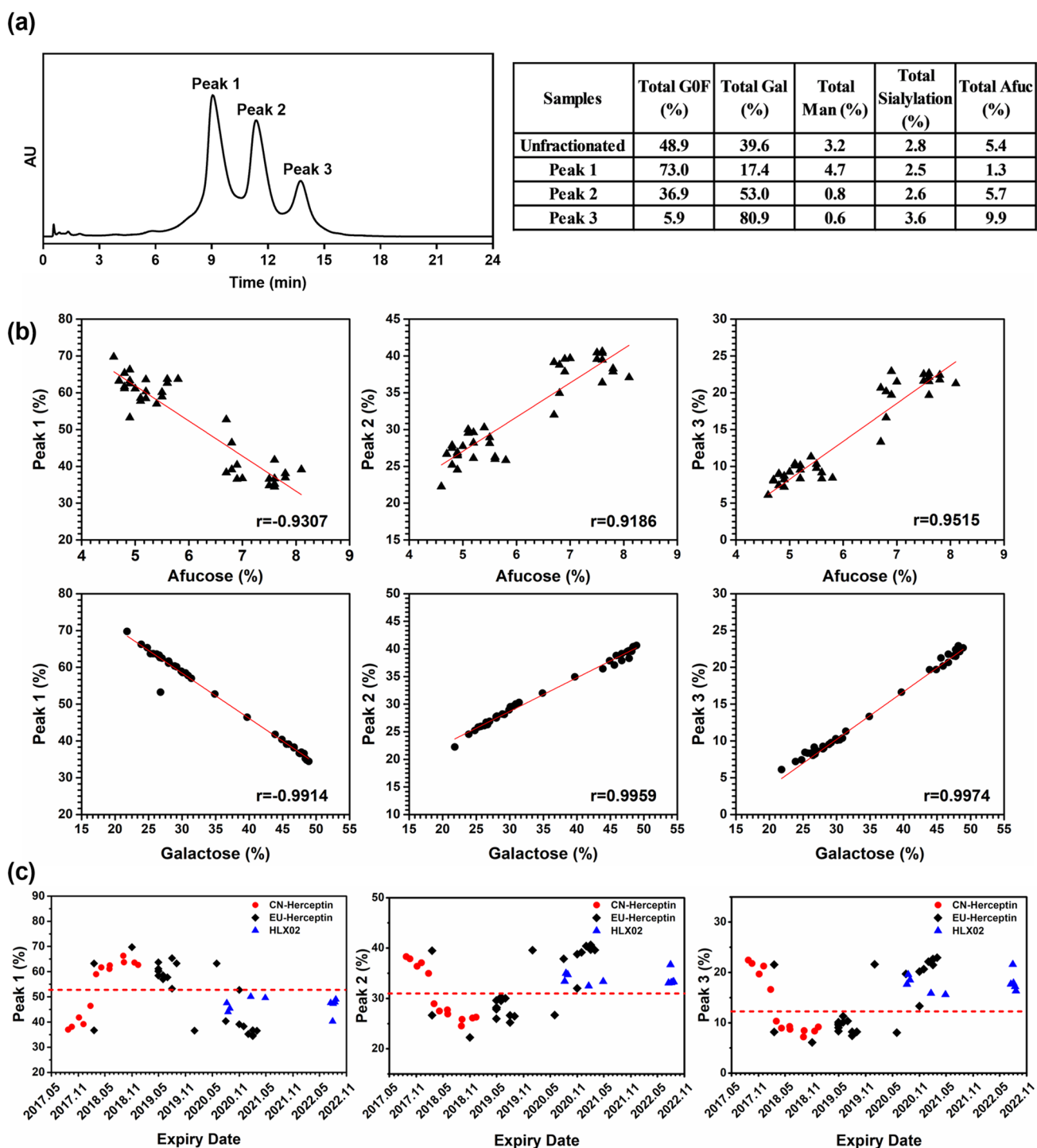


Fig. 7 Fc γ RIIIa affinity chromatographic analysis of the RPs with different expiration dates. **a** Fc γ RIIIa affinity chromatographic profile of Herceptin[®], with major glycoforms of each separated peak listed in the right table. **b** Correlation analysis between the intensity of separated peaks with the content of afucosylated and galactosylated glycans. **c** Fc γ RIIIa affinity of Herceptin[®] shift with the batch expiry date. Fc γ R Fc gamma receptor, RP reference product

rated peaks with the content of afucosylated and galactosylated glycans. **c** Fc γ RIIIa affinity of Herceptin[®] shift with the batch expiry date. Fc γ R Fc gamma receptor, RP reference product

in HLX02 has no safety concerns since it does not have the potential to cause immunogenicity as NGNA does. A series of functional assays relevant to the mechanism of action,

efficacy, and safety conducted in this study to evaluate the biological activity and immunological characteristics demonstrated that HLX02 is highly similar to CN-Herceptin[®]

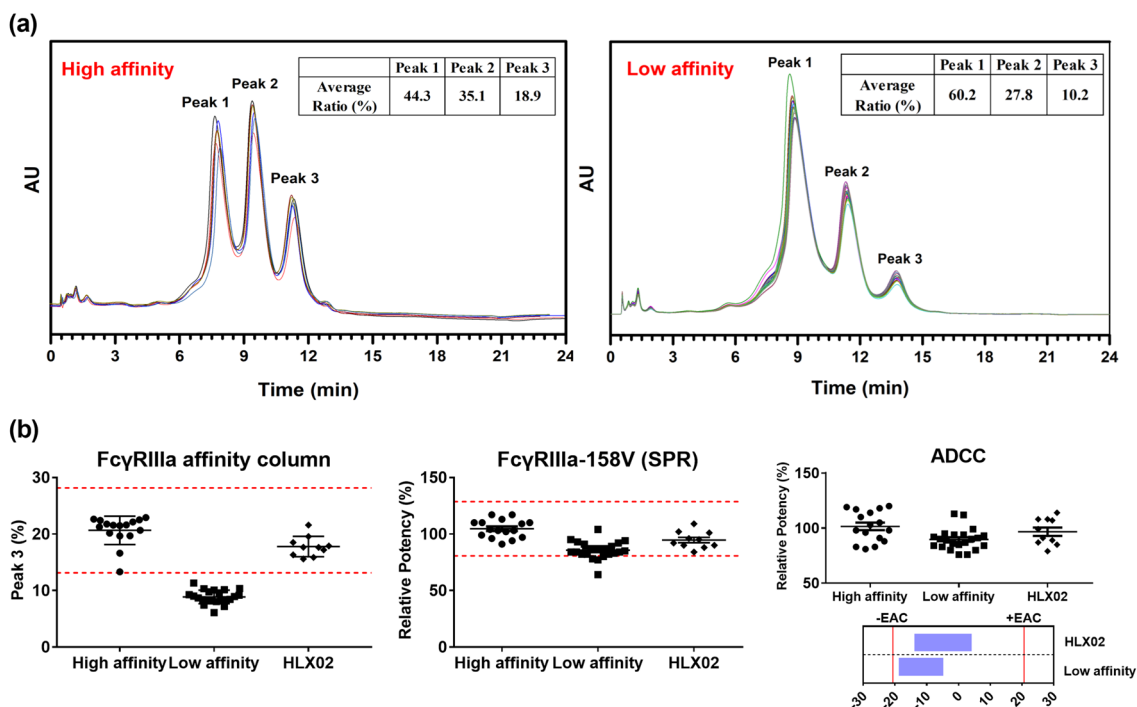


Fig. 8 Evaluation of biosimilarity between HLX02 and the RPs with FcγRIIIa affinity chromatography. **a** FcγRIIIa affinity chromatographic profiles of the RP batches with high affinity and low affinity. **b** Comparison of FcγRIIIa binding and ADCC activities for HLX02

and the RPs with low FcγRIIIa affinity or with high FcγRIIIa affinity, respectively. ADCC antibody-dependent cell-mediated cytotoxicity, FcγR Fc gamma receptor, RP reference product

and EU-Herceptin®. These addressed any potential remaining uncertainties around minor differences observed in the relative abundances of glycan, charge, and molecular size variants. In summary, the totality of evidence from physicochemical characterization, bio-functional assessments, and forced degradation studies shows that HLX02 is highly similar to the RP. There should be no clinically meaningful differences between HLX02 and Herceptin® in terms of analytical similarity, as was confirmed in clinical trials [29, 30].

Herceptin® batches with expiry dates across 5 years were included in the analytical similarity analysis, and the %afucose, %galactose, and FcγRIIIa binding activity of Herceptin® batches expiring between August 2017 and March 2021 were first down shifted, and then returned to the original levels. Due to manufacturing changes and the inherent micro-heterogeneity of therapeutic mAbs, the glycosylation pattern is often variable from one batch to another [31]. The %glycan of Herceptin® shifted every 1–2 years during the monitored expiry date period. According to the European public assessment report (EPAR) documents on the EMA website [32], the manufacturing process for the active substance of Herceptin® changed 1–3 times per year during the period 2014–2018, and it can be inferred that the glycan distribution difference may be due to one of these process changes.

FcγRIIIa affinity chromatograms revealed that the increase in %afucose and %galactose in trastuzumab enhanced affinity for FcγRIIIa, which is well known to mediate ADCC, one of the major mechanisms of action of trastuzumab. Afucosylation was reported to enhance ADCC through improved IgG binding to FcγRIIIa [17]. Glycoforms containing fucose at the base of the biantennary structure can influence the Fc three-dimensional structure and lower the binding affinity of the molecule with respect to Fc receptors such as FcγRIIIa. However, the effect of galactosylation on FcγRIIIa affinity is less clear [16]. A structure study suggested that the terminal galactose moiety could decrease the conformational entropy of CH2 and facilitate the engagement of Fc with FcγRIIIa [21]. In this study, the later-elution peaks in FcγRIIIa affinity chromatograms represent highly galactosylated antibody, reflecting an increasing affinity for FcγRIIIa. Mannosylated glycans were reported to induce ADCC via FcγRIIIa binding, but to a lesser extent than the hybrid and complex structures [33]. Sialylation may lead to decreased ADCC activity in some cases [16]. The amount of sialylated and mannosylated glycans in trastuzumab observed in this study was very low; as a result, this is unlikely to induce effector function differences.

FcγRIIIa affinity chromatography exhibited high sensitivity to changes in the FcγRIIIa affinity of trastuzumab; it

was able to discriminate between the high-affinity and low-affinity RP batches, while the affinity differences between low- and high-affinity groups could not be discriminated by SPR analysis using quality range assessment. Consistent with this observation, the lower ADCC batches reported to cause lower EFS in a previous study [13, 14] had expiry dates between August 2018 and May 2020, i.e., dates within the expiry date range of the low Fc γ RIIIa affinity group. The results demonstrated that HLX02 is highly similar to both CN-Herceptin[®] and EU-Herceptin[®], and more similar to the subgroup having a high Fc γ RIIIa affinity, with expiry dates before February 2018 or after May 2020. However, the decrease in Fc γ RIIIa binding does not result in a comparable decrease in ADCC activity, although a similar decreasing trend was observed. In addition, the binding affinity with respect to the other Fc γ Rs, FcRn, and C1q as well as the proliferation inhibition activity, CDC, and apoptosis were similar among the RP batches investigated in this study. This suggests that the use of these RP batches in clinical trials would not cause the clinical differences previously reported [15].

Taken together, using the novel Fc γ RIIIa affinity chromatography technology employed in this biosimilarity study, Herceptin[®] batches can be subgrouped into two groups: those with low Fc γ RIIIa binding affinity, with expiry dates between February 2018 and May 2020, and those with high Fc γ RIIIa binding affinity, with expiry dates before February 2018 or after May 2020. Besides having the overall analytical similarity described above, HLX02 is more similar to the RP group with high Fc γ RIIIa affinity, a result that demonstrates the power of Fc γ RIIIa affinity chromatography in biosimilarity evaluation.

Acknowledgements We gratefully thank the scientists of the Department of Bioassay and Analytical Development, Shanghai Henlius Biotech, Inc. for their assistance with experimental execution and figure preparation, as well as the Departments of Manufacturing, Quality Control, and Quality Assurance, Shanghai Henlius Biopharmaceuticals, Inc. for HLX02 manufacture and release. Shanghai Henlius Biopharmaceuticals, Inc. is a subsidiary company of Shanghai Henlius Biotech, Inc. We would also like to thank Mr. MingXiang Pan of Tosoh Bioscience Shanghai Co., Ltd. for assistance regarding the use of the Fc γ RIIIa affinity chromatography column (TSKgel FcR-IIIa-NPR).

Compliance with Ethical Standards

Funding This work was funded by Shanghai Henlius Biotech., Inc.

Conflict of interest The authors, Liqi Xie, Erhui Zhang, Yanpeng Xu, Wenyuan Gao, Linlin Wang, Michael Hongwei Xie, Peilan Qin, Lihong Lu, Sipeng Li, Pengcheng Shen, Weidong Jiang, and Scott Liu, are employees of Shanghai Henlius Biotech, and declare that they have no other conflicts of interest that might be relevant to the contents of this article.

Open Access This article is licensed under a Creative Commons Attribution-NonCommercial 4.0 International License, which permits any non-commercial use, sharing, adaptation, distribution and reproduction in any medium or format, as long as you give appropriate credit to the original author(s) and the source, provide a link to the Creative Commons licence, and indicate if changes were made. The images or other third party material in this article are included in the article's Creative Commons licence, unless indicated otherwise in a credit line to the material. If material is not included in the article's Creative Commons licence and your intended use is not permitted by statutory regulation or exceeds the permitted use, you will need to obtain permission directly from the copyright holder. To view a copy of this licence, visit <http://creativecommons.org/licenses/by-nc/4.0/>.

Reference

1. Cameron D, Piccart-Gebhart MJ, Gelber RD, Procter M, Goldhirsch A, de Azambuja E, et al. 11 years' follow-up of trastuzumab after adjuvant chemotherapy in HER2-positive early breast cancer: final analysis of the HERceptin Adjuvant (HERA) trial. *Lancet*. 2017;389(10075):1195–205.
2. Baselga J, Albanell J. Mechanism of action of anti-HER2 monoclonal antibodies. *Ann Oncol*. 2001;12(suppl 1):S35–41.
3. Organization WH. WHO model list of essential medicines: 19th list; 2015. http://www.who.int/medicines/publications/essentialmedicines/EML_2015_FINAL_amended_NOV2015.pdf?ua=1. Accessed 3 Apr 2017.
4. Blackwell K, Gligorov J, Jacobs I, Twelves C. The global need for a trastuzumab biosimilar for patients with HER2-positive breast cancer. *Clin Breast Cancer*. 2018;18(2):95–113.
5. Cortés J, Curigliano G, Diéras V. Expert perspectives on biosimilar monoclonal antibodies in breast cancer. *Breast Cancer Res Treat*. 2014;144(2):233–9.
6. Fan L, Strasser-Weippl K, Li JJ, Louis JS, Finkelstein DM, Yu KD, et al. Breast cancer in China. *Lancet Oncol*. 2014;15(7):e279–89.
7. Center for drug evaluation of China National Medical Product Administration. Technical guideline for development and evaluation of biosimilars (Interim). <http://samr.cfda.gov.cn/WS01/CL1616/115104.html>. Accessed 28 Feb 2015.
8. Committee for Medicinal Products for Human Use (CHMP) of European Medicines Agency (EMA). Guideline on similar biological medicinal products. https://www.ema.europa.eu/en/documents/scientific-guideline/guideline-similar-biological-medicinal-products-rev1_en.pdf. Accessed 23 Oct 2014.
9. Committee for Medicinal Products for Human Use (CHMP) of European Medicines Agency (EMA). Guideline on similar biological medicinal products containing biotechnology-derived proteins as active substance: quality issues (revision 1). http://www.ema.europa.eu/docs/en_GB/document_library/Scientific_guideline/2014/06/WC500167838.pdf. Accessed 22 May 2014.
10. U.S. Food and Drug Administration (FDA). Guidance for industry: Statistical approaches to evaluate analytical similarity. Accessed 22 Sep 2017.
11. U.S. Food and Drug Administration (FDA). Guidance for industry: quality considerations in demonstrating biosimilarity of a therapeutic protein product to a reference product. Accessed Apr 2015.
12. The International Council for Harmonisation of Technical Requirements for Pharmaceuticals for Human Use. Q5E comparability of biotechnological/biological products subject to changes in their manufacturing process; 2004.
13. Kim S, Song J, Park S, Ham S, Paek K, Kang M, et al. Drifts in ADCC-related quality attributes of Herceptin[®]: impact on development of a trastuzumab biosimilar. *MABs*. 2017;9(4):704–14.

14. Lee JH, Paek K, Moon JH, Ham S, Song J, Kim S. Biological characterization of SB3, a trastuzumab biosimilar, and the influence of changes in reference product characteristics on the similarity assessment. *BioDrugs*. 2019;33:411–22.
15. Pivot X, Pegram MD, Cortes J, Lüftner D, Lyman GH, Curigliano G, et al. Evaluation of survival by ADCC status: subgroup analysis of SB3 (trastuzumab biosimilar) and reference trastuzumab in patients with HER2-positive early breast cancer at three-year follow-up. *J Clin Oncol*. 2019;37(Suppl 15):580.
16. Thomann M, Reckermann K, Reusch D, Prasser J, Tejada ML. Fc-galactosylation modulates antibody-dependent cellular cytotoxicity of therapeutic antibodies. *Mol Immunol*. 2016;73:69–75.
17. Mizushima T, Yagi H, Takemoto E, Shibata-Koyama M, Isoda Y, Iida S, et al. Structural basis for improved efficacy of therapeutic antibodies on defucosylation of their Fc glycans. *Genes Cells*. 2011;16(11):1071–80.
18. Yamane-Ohnuki N, Kinoshita S, Inoue-Urakubo M, Kusunoki M, Iida S, Nakano R, et al. Establishment of FUT8 knockout Chinese hamster ovary cells: An ideal host cell line for producing completely defucosylated antibodies with enhanced antibody-dependent cellular cytotoxicity. *Biotechnol Bioeng*. 2004;87(5):614–22.
19. Thomann M, Schlothauer T, Dashivets T, Malik S, Avenal C, Bulau P, et al. In vitro glycoengineering of IgG1 and its effect on Fc receptor binding and ADCC activity. *PLoS One*. 2015;10(8):e0134949.
20. Dashivets T, Thomann M, Rueger P, Knaupp A, Buchner J, Schlothauer T. Multi-angle effector function analysis of human monoclonal IgG glycovariants. *PLoS One*. 2015;10(12):e0143520.
21. Kiyoshi M, Caaveiro JM, Tada M, Tamura H, Tanaka T, Terao Y, et al. Assessing the heterogeneity of the Fc-Glycan of a therapeutic antibody using an engineered FcγReceptor IIIa-immobilized column. *Sci Rep*. 2018;8(1):3955.
22. Wada R, Matsui M, Kawasaki N. Influence of N-glycosylation on effector functions and thermal stability of glycoengineered IgG1 monoclonal antibody with homogeneous glycoforms. *MAbs*. 2019;11(2):350–72.
23. Xu Y, Xie L, Zhang E, Gao W, Wang L, Cao Y, et al. Physicochemical and functional assessments demonstrating analytical similarity between rituximab biosimilar HLX01 and the MabThera®. *MAbs*. 2019;11(3):606–20.
24. The International Council for Harmonisation of Technical Requirements for Pharmaceuticals for Human Use. Q8(R2) Pharmaceutical development; 2009.
25. Alt N, Zhang TY, Motchnik P, Taticek R, Quarmby V, Schlothauer T, et al. Determination of critical quality attributes for monoclonal antibodies using quality by design principles. *Biologicals*. 2016;44(5):291–305.
26. U.S. Food and Drug Administration. Guidance for industry: development of therapeutic protein biosimilars: comparative analytical assessment and other quality-related considerations. <https://www.fda.gov/media/125484/download>. Accessed May 2019.
27. Harris RJ, Kabakoff B, Macchi F, Shen FJ, Kwong M, Andya JD, et al. Identification of multiple sources of charge heterogeneity in a recombinant antibody. *J Chromatogr B Biomed Sci Appl*. 2001;752(2):233–45.
28. Wang Y, Yang YJ, Wang Z, Liao J, Liu M, Zhong XR, et al. CD55 and CD59 expression protects HER2-overexpressing breast cancer cells from trastuzumab-induced complement-dependent cytotoxicity. *Oncol Lett*. 2017;14(3):2961–9.
29. Zhang Q, Xu B, Zhang Q, Sun T, Li W, Teng Y, et al. 44P Global clinical trials validating bioequivalence with China-manufactured trastuzumab biosimilar, HLX02, and trastuzumab. *Ann Oncol*. 2018;29(suppl 9):mdy428.005.
30. Xu B, Zhang Q, Sun T, Li W, Teng Y, Hu X, et al. 309PDEfficacy and safety of first China-manufactured trastuzumab biosimilar HLX02 for metastatic breast cancer: a phase III trial. *Ann Oncol*. 2019. <https://doi.org/10.1093/annonc/mdz242.004>.
31. Schiestl M, Stangler T, Torella C, Čepeljnik T, Toll H, Grau R. Acceptable changes in quality attributes of glycosylated biopharmaceuticals. *Nat Biotechnol*. 2011;29(4):310.
32. European Medicines Agency. Herceptin: EPAR—procedural steps taken and scientific information after authorisation. First published: 18/12/2008, Last updated: 27/05/2019.
33. Dietmar R, Tejada ML. Fc glycans of therapeutic antibodies as critical quality attributes. *Glycobiology*. 2015;25(12):1325–34.